

Uncertainty-resistant Stochastic MPC Approach for Optimal Operation of CHP Microgrid

Yan Zhang^a, Fanlin Meng^b, Rui Wang^{a,*}, Behzad Kazemtabrizi^c and Jianmai Shi^a

a: College of Systems Engineering, National University of Defense Technology, Changsha, 410073, PR China

b: Department of Mathematical Sciences, University of Essex, Colchester, UK CO4 3SQ

c: University of Durham, Durham, UK

* Corresponding Author ruiwangnudt@gmail.com

Abstract— The combined heat and power (CHP) microgrid can work both effectively and efficiently to provide electric and thermal power when an appropriate schedule and control strategy is provided. This study proposes a stochastic model predictive control (MPC) framework to optimally schedule and control the CHP microgrid with large scale renewable energy sources. This CHP microgrid consists of fuel cell based CHP, wind turbines, PV generators, battery/thermal energy storage system (BESS/TESS), gas fired boilers and various types of electrical and thermal loads scheduled according to the demand response policy. A mixed integer linear programming based energy management model with uncertainty variables represented by typical scenarios is developed to coordinate the operation of the electrical subsystem and thermal subsystem. This energy management model is integrated into an MPC framework so that it can effectively utilize both forecasts and newly updated information with a rolling up mechanism to reduce the negative impacts introduced by uncertainties. Simulation results show that the approach proposed in this paper is efficient when compared with an open loop based stochastic day-ahead programming (S-DA) strategy. In addition, the impacts of fuel cell capacity and TESS capacity on microgrid operations are discussed.

Keywords— stochastic model predictive control (SMPC), combined heat and power (CHP) microgrid, demand response, mixed integer linear programming (MILP)

NOMENCLATURE

<i>Index and Set</i>	
t	<i>time step index</i>
s	<i>Typical scenario index</i>
a	<i>index of electrical schedulable appliances</i>
b	<i>index of electrical shiftable appliances</i>
\mathcal{A}	<i>set of electrical schedulable appliances ($a \in \mathcal{A}$)</i>
\mathcal{B}	<i>set of electrical shiftable appliances ($b \in \mathcal{B}$)</i>
<i>Parameters</i>	
T	<i>Time length of control horizon</i>
S	<i>Number of selected typical scenarios</i>
Δt	<i>duration between two successive time intervals (h)</i>
$P_{gl}^{max}, P_{g0}^{max}$	<i>the maximum electrical power that microgrid can</i>

	<i>purchase/sell (kW)</i>
$P_{gl}^{min}, P_{g0}^{min}$	<i>the minimum electrical power that microgrid can purchase/sell (kW)</i>
$E_{BESS}^{max}, E_{BESS}^{min}$	<i>Maximum and minimum energy of electrical storage (kWh)</i>
E_{BESS}^{init}	<i>the initial energy of electrical storage (kWh)</i>
$P_{BESSc}^{max}, P_{BESSc}^{min}$	<i>the maximum, minimum charging power for electrical storage (kW)</i>
$P_{BESSd}^{max}, P_{BESSd}^{min}$	<i>the maximum, minimum discharging power for electrical storage (kW)</i>
$\eta_{BESSd}, \eta_{BESSc}$	<i>Discharging and charging efficiency of electrical storage (%)</i>
ϵ_{BESS}	<i>self-discharge of electrical storage (kWh/h)</i>
$c_{BESS}^{O\&M}$	<i>operation cost of electrical storage (\$)</i>
$E_{TESS}^{max}, E_{TESS}^{min}$	<i>Maximum and minimum energy of thermal storage (kWh)</i>
E_{TESS}^{init}	<i>the initial energy of thermal storage (kWh)</i>
$P_{TESSc}^{max}, P_{TESSc}^{min}$	<i>the maximum, minimum charging power for thermal storage (kW)</i>
$P_{TESSd}^{max}, P_{TESSd}^{min}$	<i>the maximum, minimum discharging power for thermal storage (kW)</i>
$\eta_{TESSd}, \eta_{TESSc}$	<i>Discharging and charging efficiency of thermal storage (%)</i>
ϵ_{TESS}	<i>self-discharge of thermal storage (kWh/h)</i>
$c_{TESS}^{O\&M}$	<i>operation cost of thermal storage (\$)</i>
I_a^{min}, I_a^{max}	<i>the minimum, maximum power demand of electrical schedulable appliance a (kW)</i>
T_a^{start}, T_a^{end}	<i>earliest start time, latest final time of electrical schedulable appliance a (h)</i>
E_a	<i>total energy demand of appliance a (kWh)</i>
P_{cri}^{max}	<i>maximum power of the electrical critical loads (kW)</i>
$I_{cri}(t)$	<i>power demand of electrical critical loads at time t (kW)</i>
I_b	<i>power demand of electrical shiftable appliance b (kW)</i>
T_b^{start}, T_b^{end}	<i>earliest start time, latest final time of electrical</i>

1
2
3
4
5
6
7
8
9
10
11
12
13
14
15
16
17
18
19
20
21
22
23
24
25
26
27
28
29
30
31
32
33
34
35
36
37
38
39
40
41
42
43
44
45
46
47
48
49
50
51
52
53
54
55
56
57
58
59
60
61
62
63
64
65

	<i>shift-able appliance b (h)</i>
T_b	<i>total operation time of appliance b needed (h)</i>
l_{th}^{max}	<i>the maximum power of thermal loads (kW)</i>
θ_{th}^{max}	<i>maximum curtailment ratio of thermal loads (%)</i>
l_{fl}^{max}	<i>the maximum power of electrical power flexible loads (kW)</i>
θ_{fl}^{max}	<i>maximum curtailment ratio of electrical power flexible loads (%)</i>
c_{fl}, c_{th}	<i>penalty cost efficiencies for electrical and thermal power flexible loads (\$)</i>
π^s	<i>probability of the summation power of renewable energy sources (RES) for scenario s_{pr}</i>
η_{fc}^{ele}	<i>electrical energy conversion efficiency for fuel cell</i>
μ_{fc}^{hte}	<i>heat-to-power ratio for fuel cell</i>
$P_{fc}^{ele,min}, P_{fc}^{ele,max}$	<i>Minimum and maximum electrical power output for fuel cell (kW)</i>
$T_{fc}^{on}, T_{fc}^{down}$	<i>minimum up and down time intervals for fuel cell (h)</i>
$\Delta P_{fc}^{ele,max}$	<i>rated electrical ramp power for fuel cell (kW)</i>
$c_{fc}^{om}, c_{fc}^{st}, c_{fc}^{sd}$	<i>maintenance, cold start and shut-down cost efficiency for fuel cell (\$)</i>
η_{boi}^{ther}	<i>electrical energy conversion efficiency for fuel cell</i>
$c_{boi}^{om}, c_{boi}^{st}, c_{boi}^{sd}$	<i>maintenance, cold start and shut-down cost efficiency for gas fired boiler (\$)</i>
P_{wind}^{max}	<i>rated power of wind farm (kW)</i>
P_{PV}^{max}	<i>rated power of PV plant (kW)</i>
$p^{gas}(t)$	<i>power provided by the natural gas network at time t (kW)</i>
$l_{fl}(t), l_{th}(t)$	<i>actual power flexible electrical and thermal loads at time t (kW)</i>
$p_b(t), p_s(t)$	<i>actual buying and selling electricity price at time t (\$)</i>
Forecasts	
$\hat{P}_{wind}^s(t)$	<i>power output of the wind generators at time t for scenario s (kW)</i>
$\hat{P}_{PV}^s(t)$	<i>power output of the PV generators at time t for scenario s (kW)</i>
$\hat{l}_{cri}(t)$	<i>demand of electrical critical loads at time t (kW)</i>
$\hat{l}_{fl}(t)$	<i>demand of electrical flexible loads at time t (kW)</i>
$\hat{l}_{th}(t)$	<i>demand of thermal loads at time t (kW)</i>
$\hat{p}_b(t), \hat{p}_s(t)$	<i>forecasted buying/selling electricity price at time t (\$)</i>
Decision Variables	

$P_{gl}^s(t), P_{go}^s(t)$	<i>microgrid purchased, sold power at time t under scenario s (kW)</i>
$\delta_{go}^s(t), \delta_{go}^{s'}(t)$	<i>microgrid purchasing, selling power status at time t (0/1).</i>
$P_{BESSc}^s(t), P_{BESSd}^s(t)$	<i>charging, discharging power of electrical storage at time t (kW)</i>
$\delta_{BESSc}^s(t), \delta_{BESSd}^s(t)$	<i>charging, discharging status of electrical storage at time t (0/1)</i>
$E_{BESS}^s(t)$	<i>energy level of electrical storage at time t (kWh)</i>
$P_{TESSc}^s(t), P_{TESSd}^s(t)$	<i>Charging and discharging power of thermal storage at time t (kW)</i>
$\delta_{TESSc}^s(t), \delta_{TESSd}^s(t)$	<i>charging, discharging status of thermal storage at time t (0/1)</i>
$E_{TESS}^s(t)$	<i>energy level of thermal storage at time t (kWh)</i>
$P_{fc,ele}^s(t)$	<i>electrical power output of fuel cell at time t (kW)</i>
$P_{fc,gas}^s(t)$	<i>imported gas power for fuel cell at time t (kW)</i>
$P_{fc,ther}^s(t)$	<i>thermal power output of fuel cell at time t (kW)</i>
$\delta_{fc}^s(t)$	<i>operation status of fuel cell at time t (0/1)</i>
$\delta_{fc,st}^s(t), \delta_{fc,sd}^s(t)$	<i>start-up and shut-down statuses of fuel cell at time t (0/1)</i>
$P_{boi,ther}^s(t)$	<i>thermal power output of gas fired boiler at time t (kW)</i>
$P_{boi,gas}^s(t)$	<i>imported gas power for boiler at time t (kW)</i>
$\delta_{boi}^s(t)$	<i>operation status of gas boiler at time t (0/1)</i>
$\delta_{boi,st}^s(t), \delta_{boi,sd}^s(t)$	<i>start-up, shut-down statuses of boiler at time t (0/1)</i>
$\theta_{fl}^s(t)$	<i>curtailment ratio of electrical flexible loads at time t (%)</i>
$\theta_{th}^s(t)$	<i>curtailment ratio of thermal loads at time t (%)</i>
$l_a^s(t)$	<i>load demand of schedulable appliance a at time t (kW)</i>
$\delta_a^s(t)$	<i>operation status of schedulable appliance a at time t (0/1)</i>
$\delta_b^s(t)$	<i>operation status of shiftable appliance b at time t (0/1)</i>

1. Introduction

Currently, different types of energy infrastructures, such as electricity, natural gas and heating systems are planned and operated independently [1]. On the other hand, the combined heat and power (CHP) cogeneration system can significantly improve the energy efficiency. For instance, the CHP cogeneration system efficiency is as high as 90% compared with a less than 60% efficiency for traditional electricity generation systems [2]. Among the available fuel cells (FC), internal combustion engines (ICE), and micro turbine (MT) technologies, FC-CHP and MT-CHP are preferred technologies by considering the economic profit and environmental emission

costs [3]. The 80°C to 100 °C working temperature of proton exchange membrane (PEM)-FC power plants, and their fast startup are best suited for building applications [4]. Therefore, a microgrid integrated with distributed energy resources (DERs), CHP systems and energy storage system will be a promising way to achieve an environment-friendly grid with low operation cost and high system reliability.

Along this line, a detailed mixed integer linear programming (MILP) model was proposed to minimize the short-term operation costs of a CHP microgrid in [5] where the operation cost equals to the total Operation & Maintenance (O&M) costs minus the revenue for selling electricity back to the external grid. A stochastic day-ahead scheduling strategy for a CHP microgrid with electric storage system and thermal storage system considering security constraints was proposed in [6]. In [7], a multi-objective self-scheduling optimization problem for a CHP microgrid optimal operation was studied. The considered CHP microgrid comprises energy storage systems and different types of thermal power generation units. A short-term scheduling approach of a grid-connected industrial heat and power microgrid that comprises fuel cell units, CHP generators, boiler, battery energy storage system (BESS) and heat buffer tank was studied in [8] where a probabilistic framework based on a scenario method was used to represent the uncertainties of load and price. In [9], a scenario-based mixed non-linear integer programming (MNIP) stochastic programming model was proposed to economically and optimally operate a CHP microgrid with PEMFC-CHP power plants, RESs and storages. It is worth mentioning that the above literatures are all open-loop based energy management strategies, and their performances deteriorate rapidly under a high penetration of renewable generations.

More recently, MPC has drawn much attention of the energy management community of microgrid [10][11] and multi-microgrids [12] due to that it can incorporate both forecasts and newly updated information to decide the future behaviors of system and handle different kinds of system constraints efficiently. Regarding its applications in CHP microgrid, the authors in [13] proposed an MPC based operator for heating power plant with considering fluctuating loads. The proposed approach was tested using the data obtained from a DH system. In [14], an online optimal operation approach for CCHP microgrids based on MPC with feedback correction to compensate for prediction error was investigated. In [15], an MPC based optimal control method that considers demand response was proposed to minimize the operation cost of a residential CHP microgrid. In [16], an MPC based optimal control strategy which accounts for both electrical and thermal processes in multi-building energy networks was proposed. Although MPC based approaches highly depend on the

accuracy of expected forecast data, the forecast uncertainties of single-point prediction are not considered in the aforementioned studies. Therefore, a two-stage MPC based coordinated control approach for CCHP microgrid is proposed in [17].

It is reported in [18] that stochastic approaches is able to deal with fluctuations and uncertainties with typical scenarios. In [19], an economic dispatch problem of a building Heating, Ventilation and Air Conditioning (HVAC) system was tackled with a SMPC approach. In [20], a two-layer stochastic model predictive control scheme was proposed for a microgrid to ensure probabilistic constraints satisfaction when the penetration level of renewable energy resources is high. However, many CHP microgrid key features, such as demand side programs, electrical and thermal storages, coordination of electrical and thermal networks, and ON/OFF generators status are not considered.

Therefore, a stochastic model predictive control (SMPC) based two-stage optimal scheduling strategy which combines advantages of both MPC and stochastic programming is proposed to minimize the overall operation cost of the CHP microgrid subject to relevant operation and energy balance constraints. The forecast uncertainties of wind and PV generation, load demand and electricity price are represented via typical scenarios [21]. The main contributions of this study are summarized as follows:

- A scenario-based energy management model is developed for a CHP microgrid consisting of electrical and thermal subsystems, which is formulated as a MILP problem.
- A SMPC based two-stage microgrid control framework is proposed, which includes the prescheduling stage and the power compensation stage. In the prescheduling stage, an optimal control sequence is obtained by solving the MILP based microgrid energy optimization problem, and in the power compensation stage, dispatchable units are coordinated to compensate the forecasting errors by solving a real-time economic dispatch model (REDM). The above two stages are implemented within a receding horizon control framework to consider the newly updated system and forecast information.
- A comprehensive simulation study is implemented to compare the proposed SMPC approach with the state-of-the-art methods.

The rest of this paper is organized as follows. Section 2

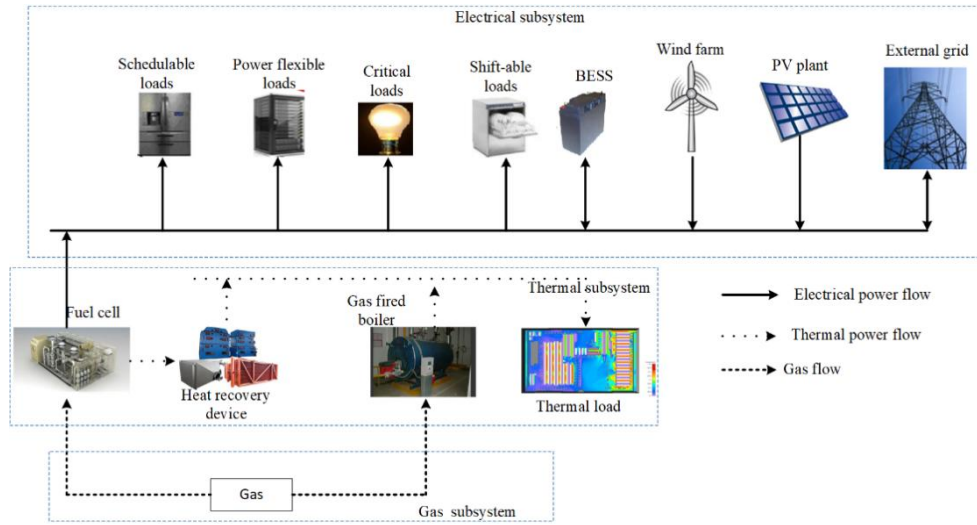


Fig. 1 Scheme of a fuel cell based CHP microgrid.

describes the problem which is to be solved. Section 3 presents the problem formulation for the CHP microgrid energy management model. Section 4 presents the SMPC based CHP microgrid control framework. Simulations are set up in Section 5. Simulation results are presented and analyzed in Section 6. Section 7 concludes this paper.

2. Problem Description

We consider a CHP microgrid, which is shown in Fig. 1. It consists of wind and PV generators, electrical and thermal storage units, power flexible, shiftable and schedulable electrical loads, fuel cells which can produce both electrical and thermal power, boilers and power flexible thermal loads.

The renewable generators can provide environment-friendly electricity power, but their power outputs are random and intermittent. Four types of electrical loads are considered in the microgrid that are shiftable loads, critical loads, power flexible loads and schedulable loads. Microgrid can purchase electrical energy from the external grid or sell electrical energy back to the external grid according to the local generation and time varying electricity prices. The fuel cell based CHP generator fires gas and provides electricity power and surplus heat power which is utilized by the heat recovery device to satisfy thermal loads. The gas fired boiler converts natural gas to thermal power. It is reckoned that the gas network can provide sufficient fuel to the fuel cell and boiler. The thermal subsystem is connected indirectly with the electrical subsystem via the fuel cell based CHP generator. The control inputs of each time period (i.e. one hour considered in this study) are obtained by solving an MILP based microgrid operation optimization problem to be presented in Section 3.

The decision variables include the electrical/thermal power output of the CHP and boiler, the charge/discharge power of electrical and thermal storages, the operation power of flexible thermal and electrical loads, the operation time of shiftable and schedulable loads, the power exchange between the microgrid and external grid, and the gas inputs for boiler and CHP.

3. Microgrid Energy Management

The forecast errors of load demand, wind production, PV generation and electricity price are all considered to follow Gaussian distribution [22] [23]. In order to account for the forecast uncertainties, a large number of primary scenarios are firstly generated using the Lattice Monte Carlo Simulation method (LMCS) [24]. To improve the computational tractability, a scenario reduction technique based on the simultaneous backward scenario reduction (SBSR) method [25] is utilized to select several representative scenarios from those primary scenarios.

Note that in this study we are focusing on the scenario-based microgrid energy management and SMPC framework rather than developing new methods for scenario generation and scenario reduction. The details of the scenario generation and scenario reduction procedures adopted in this study can be found in the above referenced literatures.

The energy management problem for the microgrid within the control horizon can be modeled as an MILP problem. The control horizon is divided into T time intervals ($t \in [1, 2, \dots, T]$) where the time duration of each time interval is defined as Δt .

3.1 Objective function

The objective function (1) of microgrid energy management system (EMS) is to minimize the operation cost of all typical power scenarios and all dispatchable units over the control horizon. Specifically, the overall cost consists of the cost of purchasing electricity and natural gas, and the selling electricity revenue; the O&M cost for fuel cell generator and boiler (including the maintenance cost, cold start cost, and shut-down cost); the deregulation cost for electrical and thermal storages due to frequent discharging and charging; penalty cost of comfort loss due to curtailment of power flexible electrical and thermal loads.

$$\begin{aligned}
\min \sum_{s=1}^S \pi^s \sum_{t=1}^T \{ & P_{gt}^s(t) \hat{p}_b(t) \Delta t - P_{go}^s(t) \hat{p}_s(t) \Delta t \\
& + [c_{fc}^{om} \delta_{fc}^{ele}(t) + P_{fc}^{gas}(t) p_{gas}(t) \Delta t \\
& + c_{fc}^{st} \delta_{fc, st}^s(t) + c_{fc}^{sd} \delta_{fc, sd}^s(t)] \\
& + [c_{boi}^{om} \delta_{boi}^s(t) + P_{boi, gas}^s(t) p_{gas}(t) \Delta t \\
& + c_{boi}^{st} \delta_{boi, st}^s(t) + c_{boi}^{sd} \delta_{boi, sd}^s(t)] \\
& + c_{BESS}^{O\&M} (P_{BESSc}^s(t) + P_{BESSd}^s(t)) \Delta t \\
& + \hat{l}_{f1}(t) \theta_{f1}^s(t) c_{f1} \Delta t + \hat{l}_{th}(t) \theta_{th}^s(t) c_{th} \Delta t \}
\end{aligned} \quad (1)$$

3.2 CHP operation constraints

Fuel cell-based CHP generator converts natural gas into a hydrogen-rich feed stream and provides both heat and electricity to the microgrid [26]. Since the heat generated by the fuel cell is collected and output by heat recovery devices, the fuel cell must operate coordinately with them [9]. This study assumes the fuel cell and heat recovery devices are integrated in the CHP unit and therefore are considered as one single unit.

$$P_{fc, ele}^s(t) = \eta_{fc}^{ele} P_{fc, gas}^s(t) \quad (2)$$

$$P_{fc, ther}^s(t) = \mu_{fc}^{hte} P_{fc, ele}^s(t) \quad (3)$$

$$P_{fc}^{ele, min}(t) \leq P_{fc, ele}^s(t) \leq P_{fc}^{ele, max}(t) \quad (4)$$

$$-\Delta P_{fc}^{ele, max} \leq P_{fc, ele}^s(t) - P_{fc, ele}^s(t-1) \leq \Delta P_{fc}^{ele, max} \quad (5)$$

$$\delta_{fc}^s(t) - \delta_{fc}^s(t-1) \leq \delta_{fc}^s(\tau_{fc1}) \quad (6)$$

$$\delta_{fc}^s(t-1) - \delta_{fc}^s(t) \leq 1 - \delta_{fc}^s(\tau_{fc2}) \quad (7)$$

$$\delta_{fc}^s(t) - \delta_{fc}^s(t-1) \leq \delta_{fc, st}^s(t) \quad (8)$$

$$\delta_{fc}^s(t-1) - \delta_{fc}^s(t) \leq \delta_{fc, sd}^s(t) \quad (9)$$

The electrical and thermal power outputs of fuel cell for each time period and scenario are denoted in (2) and (3), respectively. The technical constraint of fuel cell on electrical output modulation is shown in (4). The ramp power constraints are described in (5). The minimum up and down time constraints are expressed in (6) and (7), respectively where $\tau_{fc1} = t + 1, \dots, \min(t + T_{fc}^{on} - 1, T)$ and $\tau_{fc2} = t + 1, \dots, \min(t + T_{fc}^{down} - 1, T)$. The fuel cell cold starts and shuts down actions are considered in (8) and (9), respectively.

3.3 Boiler operation constraints

Boiler's thermal output equals to the imported natural gas power multiplied by the conversion efficiency η_{boi}^{ther} , as shown in (10). Power output constraints of boiler are shown in (11). The starting up and shutting down actions are tracked in (6) and (7), respectively.

$$P_{boi, ther}^s(t) = \eta_{boi}^{ther} P_{boi, gas}^s(t) \quad (10)$$

$$P_{boi}^{min}(t) \leq P_{boi, ther}^s(t) \leq P_{boi}^{max}(t) \quad (11)$$

$$\delta_{boi}^s(t) - \delta_{boi}^s(t-1) \leq \delta_{boi, st}^s(t) \quad (12)$$

$$\delta_{boi}^s(t-1) - \delta_{boi}^s(t) \leq \delta_{boi, sd}^s(t) \quad (13)$$

3.4 BESS operation constraints

Among all storage technologies, the battery energy storage system (BESS) is shown as a suitable choice for integrating DERs. The battery dynamics is modelled in (8), which considers both conversion efficiency and self-discharging rate. The battery storage energy level, charging power and discharging power should be bounded in its technical specifications, which are reflected in (9), (10) and (11), respectively. To avoid simultaneously charge and discharge actions of the battery storage units, (12) is enforced.

$$E_{BESS}^s(t+1) = E_{BESS}^s(t) + \eta_{BESSc} P_{BESSc}^s(t) \Delta t - 1/\eta_{BESSd} P_{BESSd}^s(t) \Delta t - \varepsilon_{BESS} \quad (14)$$

$$E_{BESS}^{min} \leq E_{BESS}^s(t+1) \leq E_{BESS}^{max} \quad (15)$$

$$\delta_{BESSc}^s P_{BESSc}^{min} \leq P_{BESSc}^s(t) \leq \delta_{BESSc}^s(t) P_{BESSc}^{max} \quad (16)$$

$$\delta_{BESSd}^s(t) P_{BESSd}^{min} \leq P_{BESSd}^s(t) \leq \delta_{BESSd}^s(t) P_{BESSd}^{max} \quad (17)$$

$$\delta_{BESSc}^s(t) + \delta_{BESSd}^s(t) \leq 1 \quad (18)$$

In addition, the energy level of BESS at the beginning of each day is reset to its initial level, which enables the energy storage system has enough energy stored to deal with unforeseen emergency conditions and is commonly adopted in relevant studies

3.5 TESS operation constraints

Like the BESS, the thermal energy storage system (TESS) dynamics is expressed in (139). Its energy level, charging power and discharging power constraints are given in (20), (21), and (22). The TESS unit cannot charge and discharge simultaneously as defined in (14). For the same reason as BESS, the energy level of TESS at the beginning of each day is reset to the initial state.

$$E_{TESS}^s(t+1) = E_{TESS}^s(t) + \eta_{TESSc} P_{TESSc}^s(t) \Delta t - 1/\eta_{TESSd} P_{TESSd}^s(t) \Delta t - \varepsilon_{TESS} \quad (19)$$

$$E_{TESS}^{min} \leq E_{TESS}^s(t+1) \leq E_{TESS}^{max} \quad (20)$$

$$\delta_{TESSc}^s P_{TESSc}^{min} \leq P_{TESSc}^s(t) \leq \delta_{TESSc}^s(t) P_{TESSc}^{max} \quad (21)$$

$$\delta_{TESSd}^s(t) P_{TESSd}^{min} \leq P_{TESSd}^s(t) \leq \delta_{TESSd}^s(t) P_{TESSd}^{max} \quad (22)$$

$$\delta_{TESSc}^s(t) + \delta_{TESSd}^s(t) \leq 1 \quad (23)$$

3.6 Loads and RES limits

According to the classification of loads in the smart grid [15], there are four types of electrical loads: critical loads, power flexible loads, shiftable loads and schedulable loads. All thermal loads in microgrid are considered as power flexible loads.

The forecast and actual demand of electrical critical loads must be bounded within its technical specifications, as shown in (15).

$$0 \leq \hat{l}_{cri}(t) \leq l_{cri}^{max} \quad (24)$$

Demand of the electrical and thermal power flexible loads can be curtailed by users. Similar to critical loads, their

forecasted and actual demand is bounded within their technical specifications [10]. Furthermore, their curtailments should also be bounded, as shown in (165) and (17).

$$0 \leq \theta_{fl}^s(t) \leq \theta_{fl}^{max} \quad (25)$$

$$0 \leq \theta_{th}^s(t) \leq \theta_{th}^{max} \quad (26)$$

Shiftable loads are flexible within the time window but their demands cannot be adjusted, as shown in (187), and they cannot work earlier than the earliest start time or later than the latest finish time, as shown in (198). In addition, once their work is started, they cannot be stopped until the completion, as shown in (209).

$$\sum_{t=T_b^{start}}^{T_b^{end}} \delta_b^s(t) = T_b, b \in B \quad (27)$$

$$\sum_{t=1}^{T_b^{start}-1} \delta_b^s(t) + \sum_{t=T_b^{end}+1}^T \delta_b^s(t) = 0, b \in B \quad (28)$$

$$\sum_{t=t}^{T_b+t} \delta_b^s(t) \geq T_b(\delta_b^s(t) - \delta_b^s(t-1)), t \in [T_b^{start}, T_b^{end} - T_b], b \in B \quad (29)$$

Schedulable loads can not only adjust the operation time, as shown in (30) and (31), but also can adjust the operation power (21). However, the total power demand must be satisfied before completing the task (22).

$$\sum_{t=T_a^{start}}^{T_a^{end}} \delta_a^s(t) = T_a, a \in A \quad (30)$$

$$\sum_{t=t}^{T_a+t} \delta_a^s(t) \geq T_a(\delta_a^s(t) - \delta_a^s(t-1)), t \in [T_a^{start}, T_a^{end}], a \in A \quad (31)$$

$$l_a^{min} \delta_a^s(t) \leq l_a^s(t) \leq l_a^{max} \delta_a^s(t), a \in A \quad (32)$$

$$\sum_{t=T_a^{start}}^{T_a^{end}} l_a^s(t) \Delta t = E_a^s, a \in A \quad (33)$$

Therefore, the total electrical load demand at time t for scenario s can be expressed as $l_{ele}^s(t)$ in (23).

$$l_{ele}^s(t) = \sum_{a=1}^A l_a^s(t) + \sum_{b=1}^B l_b^s \delta_b^s(t) + \hat{l}_{fl}(t)(1 - \theta_{fl}^s(t)) + \hat{l}_{cri}(t) \quad (34)$$

Similar to the critical loads, constraints of the forecast and actual power outputs of RES are shown in (24) and (25). $P_{renew}^s(t)$ is the summation of power generated by RES, as shown in (26).

$$0 \leq \hat{P}_{pv}^s(t) \leq P_{pv}^{max} \quad (35)$$

$$0 \leq \hat{P}_{wind}^s(t) \leq P_{wind}^{max} \quad (36)$$

$$P_{renew}^s(t) = \hat{P}_{wind}^s(t) + \hat{P}_{pv}^s(t) \quad (37)$$

3.7 Microgrid exchange limits

In deregulated electricity market, buying and selling price for the same time slot may be different. Meanwhile, the external grid may limit the minimum and maximum buying/selling power of the microgrid. To better express such purchasing/selling electricity behaviors of the microgrid, the following power exchange model is adopted.

$$P_{gl}^{min} \delta_{gl}^s(t) \leq P_{gl}^s(t) \leq P_{gl}^{max} \delta_{gl}^s(t) \quad (38)$$

$$P_{go}^{min} \delta_{go}^s(t) \leq P_{go}^s(t) \leq P_{go}^{max} \delta_{go}^s(t) \quad (39)$$

$$\delta_{go}^s(t) + \delta_{gl}^s(t) \leq 1 \quad (40)$$

Eqs. (27) and (28) indicate that the power bought/sold by the microgrid must be bounded by its technical specifications. Eq. (40) is imposed to ensure that the microgrid cannot buy and sell power, simultaneously.

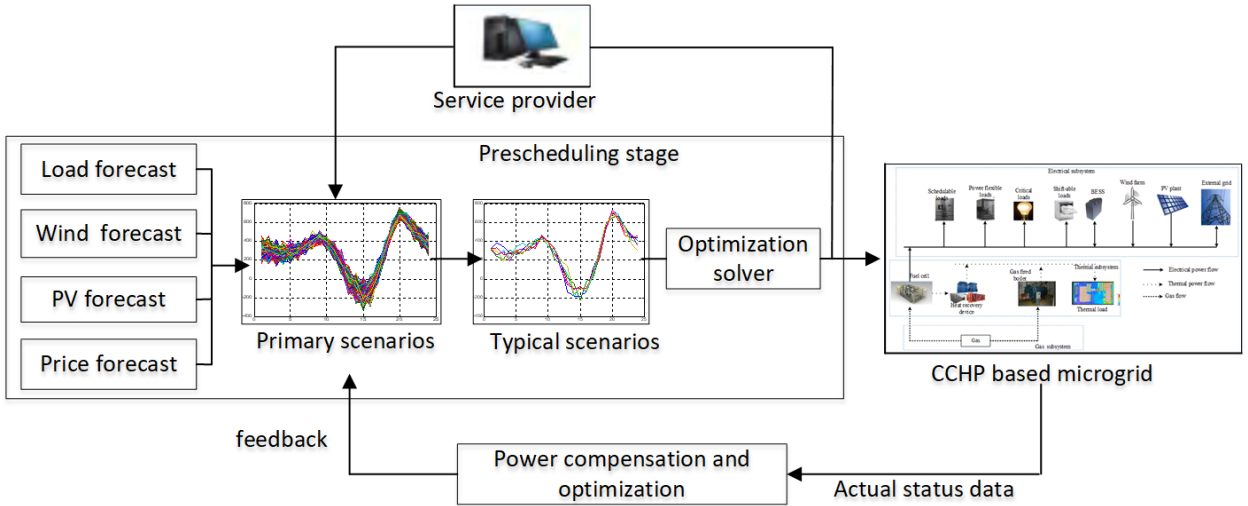


Fig. 2 Framework of SMPC control strategy for microgrid.

3.8 Power balance limits

For each time interval and scenario, the power balance constraints for thermal subsystem (41), electrical subsystem (29) and gas subsystem (30) must be satisfied. In addition, the gas demand of the microgrid is assumed to be met by the gas subsystem.

$$P_{gl}^s(t) - P_{go}^s(t) = l_{ele}^s(t) - (P_{BESSa}^s(t) - P_{BESSc}^s(t)) - P_{fc,ele}^s(t) - P_{renew}^s(t) \quad (41)$$

$$\mu_{fc}^{hte} P_{fc,ele}^s(t) + P_{boi,ther}^s(t) = (1 - \theta_{th}^s(t)) \hat{l}_{th}(t) \quad (42)$$

$$P_{fc,gas}^s(t) + P_{boi,gas}^s(t) = P_{gas}^s(t) \quad (43)$$

4. SMPC Control Framework

Traditional open-loop based energy control strategy deteriorates rapidly when the penetration level of RESs in microgrid grows high [27]. Although MPC based closed-loop strategies operate based on expected RESs forecast, they cannot handle forecast uncertainties effectively. Therefore, this paper proposes a stochastic model predictive control (SMPC) [28] based strategy to optimally schedule and control the CHP microgrid with RESs. The SMPC combines advantages of both stochastic programming and MPC, which therefore is more suitable to our problem.

To ensure reliable and efficient microgrid operations, a two-stage SMPC based microgrid energy management model consisting of the prescheduling stage and the power compensation stage is proposed as illustrated in Fig. 2.

The scenario based microgrid energy management model in Section 3 can be seen as a base model, which will be used to define the pre-scheduling stage optimization model. In the following, the problem formulations of the prescheduling stage and the power compensation stage are firstly given. Second, a formal SMPC algorithm which links together both the prescheduling stage and power compensation optimizations within a rolling horizon framework.

4.1 Prescheduling stage

Define the current time period t , the prescheduling stage optimization aims to obtain a control sequence for a future horizon of T time periods by solving Eq. (1) over time periods from $t + 1$ to $t + T$ (inclusive) with relevant constraints.

The constraints include Eqs. (2)-(43) defined in Section 3. Since the control action in the next time period ($t + 1$) under different scenarios must be the same to be actually operated [28], the following additional non-anticipation constraints Eqs. (44)–(55) for time period $t + 1$ must be included in the prescheduling stage optimization model.

$$P_{fc,ele}^s(t+1) = P_{fc,ele}^{s+1}(t+1) \quad (44)$$

$$P_{BESSc}^s(t+1) = P_{BESSc}^{s+1}(t+1) \quad (45)$$

$$P_{BESSd}^s(t+1) = P_{BESSd}^{s+1}(t+1) \quad (46)$$

$$P_{gl}^s(t+1) = P_{gl}^{s+1}(t+1) \quad (47)$$

$$P_{go}^s(t+1) = P_{go}^{s+1}(t+1) \quad (48)$$

$$\theta_{fl}^s(t+1) = \theta_{fl}^{s+1}(t+1) \quad (49)$$

$$l_b^s(t+1) = l_b^{s+1}(t+1), b \in B \quad (50)$$

$$l_a^s(t+1) = l_a^{s+1}(t+1), a \in A \quad (51)$$

$$\theta_{th}^s(t+1) = \theta_{th}^{s+1}(t+1) \quad (52)$$

$$P_{TESSc}^s(t+1) = P_{TESSc}^{s+1}(t+1) \quad (53)$$

$$P_{TESSd}^s(t+1) = P_{TESSd}^{s+1}(t+1) \quad (54)$$

$$P_{boi,ther}^s(t+1) = P_{boi,ther}^{s+1}(t+1) \quad (55)$$

Finally, the prescheduling stage optimization problem is defined by minimizing objective in Eq. (1) with constraints Eqs. (2)-(55).

4.2 Power compensation stage

As aforementioned, at time period t , a prescheduling stage optimization problem is solved over time periods from $t + 1$ to $t + T$. Since the forecasts and actual system states are usually mismatching, when time comes to $t + 1$, the control action obtained for $t + 1$ based on forecasts information in the pre-scheduling stage is likely to result in a mismatch between demand and supply when the actual load demand and RESs data become available. As a result, real-time adjustments are needed to guarantee the power balance in the system. To this end, in this paper a real-time economic dispatch model (REDM) model is developed as an optimal power compensation solution to obtain optimal adjustment control actions of dispatchable units to match demand and supply in real-time. The REDM is given by Eq. (56).

$$\begin{aligned} \min & \left(P'_{BESSc}(t+1) + P'_{BESSd}(t+1) \right) c_{BESS}^{O\&M} \Delta t \\ & + \left(P'_{TESSc}(t+1) \right. \\ & + P'_{TESSd}(t+1) \left. \right) c_{TESS}^{O\&M} \Delta t \\ & + P'_{gridl}(t+1) p_b(t+1) \Delta t \\ & - P'_{grido}(t+1) p_s(t+1) \Delta t \\ & + P'_{boi,gas}(t+1) p_{gas}(t+1) \Delta t \\ & + \theta'_{fl}(t+1) l_{fl}(t+1) c_{fl} \Delta t \\ & + \theta'_{ther}(t+1) l_{ther}(t+1) c_{ther} \Delta t \end{aligned} \quad (56)$$

The optimization variables of Eq. (56) include:

- $P'_{BESSc}(t+1)/P'_{BESSd}(t+1)$: adjusted charge/discharge power of BESS;
- $P'_{TESSc}(t+1)/P'_{TESSd}(t+1)$: adjusted charge/discharge power of TESS;
- $P'_{boi,gas}(t+1)$: adjusted power outputs of boiler;
- $P'_{gridl}(t+1)/P'_{grido}(t+1)$: adjusted purchasing and selling power of the microgrid
- $\theta'_{fl}(t+1)/\theta'_{ther}(t+1)$: adjusted power curtailment ratio of power flexible electrical and thermal loads.

Eq. (56) aims to compensate the power supply/demand forecast error with the minimum cost. Since the optimal control adjustments of Eq. (56) are obtained based on the optimization results (control sequence) in the prescheduling stage, no significant power adjustment greater than forecast errors is implemented. Therefore, if the forecast error is not very large, the CHP generator will not take part in the power compensation stage operation due to that its adjustment could affect both electrical and thermal subsystems. Finally, the resulted control actions after adjustment for $t + 1$ are applied to the system.

4.3 SMPC algorithm

Based on the optimization models defined for the

prescheduling stage and the power compensation stage, the detailed operation steps of our proposed SMPC framework are given below where Steps 2 – 5 will be repeated till the end of the simulation horizon.

1) Initialize simulation starting time $t \leftarrow 0$.

2) **The prescheduling stage:** by the end of time period t , a control sequence between time period $t + 1$ and $t + T$ is obtained by solving the prescheduling stage optimization problem defined in subsection 4.1.

3) **The power compensation stage:** at the beginning of period $t + 1$, the optimal adjustment control actions of dispatchable units are obtained by solving the real-time economic dispatch model (REDM) Eq. (56) defined in subsection 4.2. Finally, the resulted control actions after adjustment for time period $t + 1$ are applied to the system.

4) **The final microgrid operation state updates:** actual RES outputs data, electrical and thermal load data, and electricity price data in time period $t + 1$ are sent to the microgrid EMS to update the forecast model and energy management optimization model.

5) $t \leftarrow t + 1$, go to Step 2.

5. Case setup

The proposed approach is applied to a hypothetical CHP microgrid as shown in Fig.1. This microgrid is worked in grid-connected mode, and comprises PV panels, wind turbines, a BESS unit, a TESS unit, a fuel cell based CHP generator, a boiler and various types of thermal and electrical loads.

Related details of the microgrid are summarized as follows.

- The rated capacity of the PV and wind turbines are 500 kW and 700 kW, and the history data of PV and wind are collected and modified from ELIA [29].
- The rated capacity of BESS is 800 kWh with the depth of charge of 0.75, and the maximum and minimum operation power of 300 kW and 5 kW, respectively. The rated capacity of TESS is 400 kWh with the depth of charge of 0.85, and the maximum and minimum operation power of 200 kW and 0 kW, respectively. Other BESS and TESS parameters are adopted from [30].
- The rated electrical power of CHP is 600kW with the minimum power output of 40kW. The rated ramp power is 300 kW, and the electrical output efficiency is 0.38. The heat-to-power rate is considered to be 1.2. In addition, the minimum up time is 3 hours, and the maximum down time is 2 hours. The natural gas price is considered at 0.06\$/kWh.
- The rated power of boiler is 440kW with the minimum

power output of 20 kW and the output efficiency of 0.76. The ramp power is 300 kW, and the natural gas price is 0.15\$/kWh.

- The critical and power flexible loads data are collected and modified from ELIA [29]. Thermal load demand data are generated by the versatile energy resource allocation (VERA) software [33]. The maximum curtailment ratio for the thermal and electrical loads are 0.4 and 0.3 respectively, and the penalty coefficients for curtailing thermal/electrical flexible loads are 1.8. In addition, the shiftable and schedulable loads parameters are shown in Tables I and II, respectively.
- Electricity price data are collected and modified from [32]. In order to incentivize the use of RESs locally, the electricity purchasing price in the power compensation stage is higher than the prescheduling stage whereas the selling price is the opposite case [31]. The maximum purchasing and selling power for the microgrid are 1000 kW and -1000 kW respectively. The history data of RES power generation (PV and wind), planned electricity net-load (RES power minus all electrical loads), thermal loads and electricity price are shown in Fig.3.

Note that the net-load data in Fig.3 indicate that the planned microgrid net-load demand exceeds the power exchange limit (i.e. greater than 1000kW) in some time slots whilst in some other time slots the RES generation is larger than the microgrid electrical load demand. As a result, it is important for the microgrid to have enough flexibility in order to guarantee the system's safety and reliability. In the next section, we will demonstrate how our proposed CHP microgrid energy management model could provide such system flexibilities.

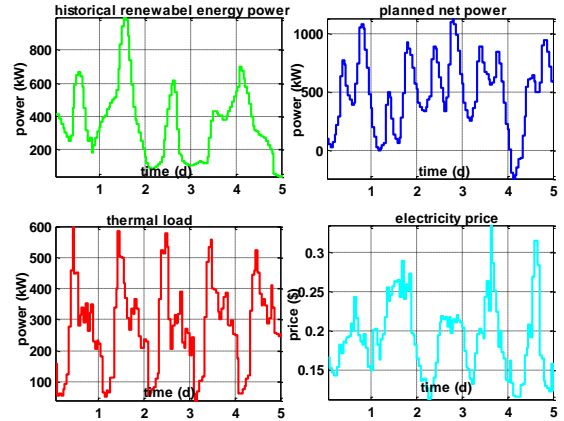


Fig. 3 History data of the microgrid.

Table 1. Parameter of shiftable loads

Shift-able load	Power (kW)	Time window (h)	Duration (h)
SF-Task 1	28	10-20	4
SF-Task 2	45	6-18	6

<i>SF-Task 3</i>	35	12-23	5
<i>SF-Task 4</i>	16	4-22	9

Table 2. Parameter of schedulable loads

<i>Schedulable load</i>	Base power	Max, Min power	Time window	Duration
<i>SC-Task 1</i>	80	25, 150	2-18	5
<i>SC-Task 2</i>	25	5, 50	2-20	8
<i>SC-Task 3</i>	55	20, 80	5-22	6
<i>SC-Task 4</i>	40	10, 60	3-21	12

The proposed SMPC approach is compared with an open loop based stochastic day-ahead programming (SDA) strategy [34] which also consists of two stages. In the prescheduling stage, the energy storage operation schedule, shiftable loads and schedulable loads operation schedules, and operation statuses of CHP units are determined at the beginning of each day with forecasting uncertainties represented by typical scenarios. In the power compensation stage, a REDM will be constructed and solved to dispatch relevant units.

6. Results and Analysis

In this section, simulation results are presented to demonstrate the superiority of our proposed SMPC over the frequently often used S-DA approach and the single-stage MPC approach. In addition, as two important components in the CHP microgrid, the impacts of the fuel cell capacity and TESS capacity on the microgrid operations and costs are investigated.

6.1 Microgrid operation comparison

Fig.4 shows the results of microgrid exchange powers for SMPC strategy, MPC strategy and SDA strategy in prescheduling stage and real-time operation stage. The green line is the microgrid purchasing/selling power when no optimization strategy is implemented, which serves as the benchmark. It indicates that no matter which optimization strategy is implemented, the prescheduled and actual power exchanges between the microgrid and the external grid do not exceed the maximum power exchange capacity, in contrast to the benchmark. In addition, compared with the SDA strategy, better optimization schedules are planned in the prescheduling stage and less power compensation adjustments are implemented in the real-time power compensation stage for both the SMPC and MPC strategies. Since the SDA strategy is an open-loop based optimization strategy, its REDM only considers the current time-step system data rather than a look-ahead and rolling horizon mechanism as in the SMPC and MPC strategies. The total power mismatch between the prescheduling stage and real-time compensation stage for the SDA strategy is 1019.9kWh, which is much larger than the 143.45kWh for the SMPC strategy and the 307.38kWh for the MPC strategy. In addition, compared with the MPC strategy, the optimization in the prescheduling stage for the SMPC strategy considers more uncertainty factors, which results in

that the SMPC strategy purchases more power from the external grid than the MPC strategy. Fig.5 shows the operation routines of schedulable loads and shiftable loads for these three strategies. Note that due to the operational constraints, shiftable loads and schedulable loads do not take part into the real-time power compensation stage operation. Even though, these controllable loads can still improve the microgrid flexibility by adjusting their operation time /operation power compared with the benchmark. As can be seen in Fig.5, the operation schedules of these three strategies are also different: 1) the SMPC strategy is a little conservative; 2) schedulable loads are more flexible than the shiftable loads since they can be adjusted in terms of both the operation power and operation time.

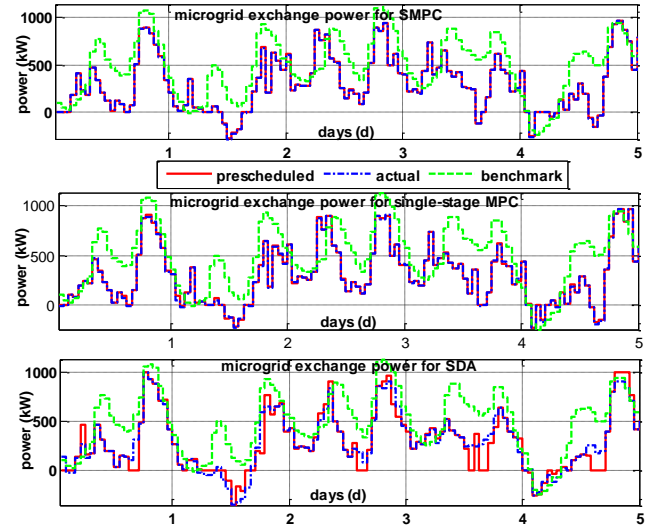


Fig. 4 Microgrid purchasing/selling power for SMPC, MPC and SDA strategy

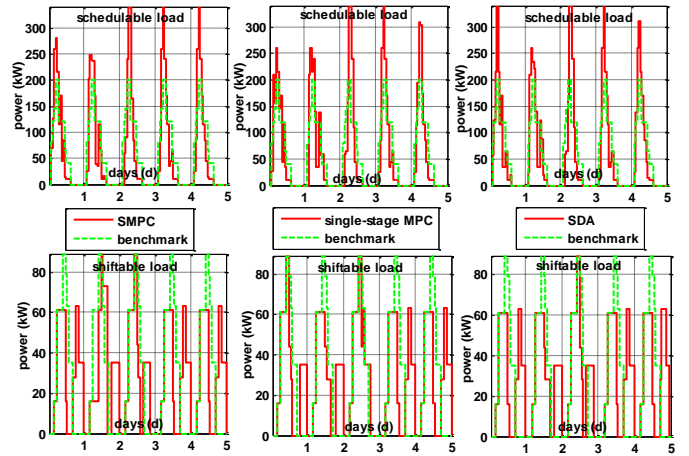


Fig. 5 Operation schedule of schedulable loads and shift-able loads SMPC and SDA strategy

Fig.6 shows that the electrical power outputs of fuel cell generator in prescheduling stage and real-time power compensation stage for the SMPC strategy and the MPC strategy respectively as well as electric power outputs of fuel cell generator in real-time power compensation stage for the

SDA strategy. Note that for the SDA strategy, only the on/off status variables are determined in the prescheduling stage whereas the final power outputs are determined by taking into consideration of the actual RESs generation data, load demand data and the selling/buying electricity price data (i.e., in the real-time power compensation stage). As we all know, the fuel cell generator not only can produce heat to satisfy the heat demand but also can supply electrical energy to satisfy electrical demand, therefore the surplus electrical or/and thermal energy can be stored by BESS or/and TESS systems. In Fig.6, the total power output difference between the SMPC strategy and the MPC strategy is 1174.6kWh whereas the total power output difference between the SMPC strategy and the SDA strategy is 5121.8kWh. The mismatch between the actual power production and scheduled power production in the prescheduling stage for the SMPC strategy is greater than 21.54kWh. However, this power production difference is 84.9kWh.

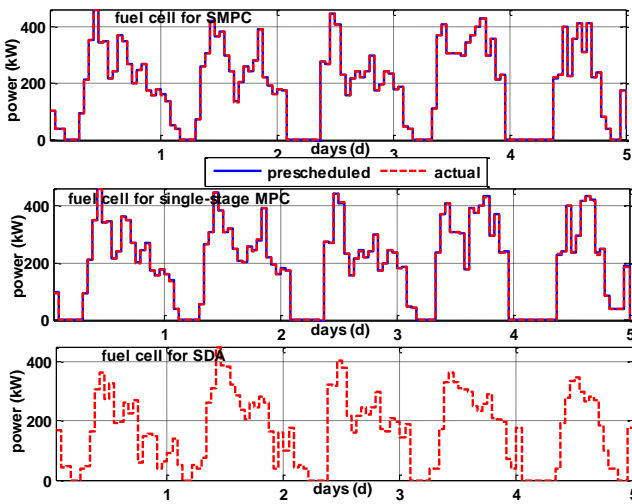


Fig. 6 Operation schedule of CHP generator

Fig.7 shows the BESS and TESS operation routines for the SMPC strategy, the MPC strategy and the SDA strategy. The positive value represents the discharge power while the negative value represents the charge power. The coordination of energy storage devices and thermal or/and electrical generators can not only improve the flexibility of microgrid system but also the microgrid economics. However, comparing to the rolling horizon based SMPC strategy and MPC strategy, the SDA strategy does not full play the advantages of the storage devices due to the near-sight of real-time operation of the SDA strategy. Over the simulation horizon, the BESS charges and discharges in total around 4744.2kWh, 4601.8kWh and 210.53kWh for the SMPC strategy, the MPC strategy and the SDA strategy, respectively; the TESS charges and discharges around 5067.8kWh, 4808.6kWh and 63.83kWh for the SMPC strategy, the MPC strategy and the SDA strategy, respectively.

Fig.8 shows the boiler operation routines for the SMPC strategy, the MPC strategy and the SDA strategy. Since the

thermal load demand cannot be perfect forecasted and the power shift advantages of the TESS is not fully displayed under the SDA strategy. This results in that the boiler generates much more thermal energy under SDA strategy than its counterparts. To be specific, the boiler generates 3401.7kWh, 3601.9kWh and 7849.6kWh for the SMPC strategy, the MPC strategy and the SDA strategy, respectively.

Thanks to the fact that the considered microgrid has sufficient capability to produce electrical and thermal power to meet the demand and deal with forecast uncertainties, there are no curtailments of electrical and thermal power flexible loads. However, in situations that there is insufficient generation due to e.g., generator failures, these power flexible loads can still be curtailed to maintain the system stability.

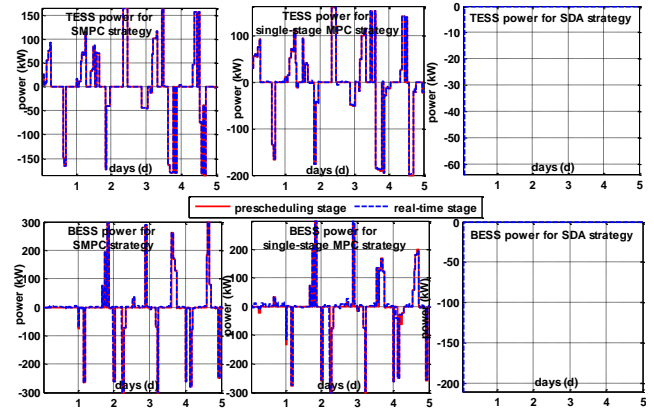


Fig. 7 Operation of BESS and TESS

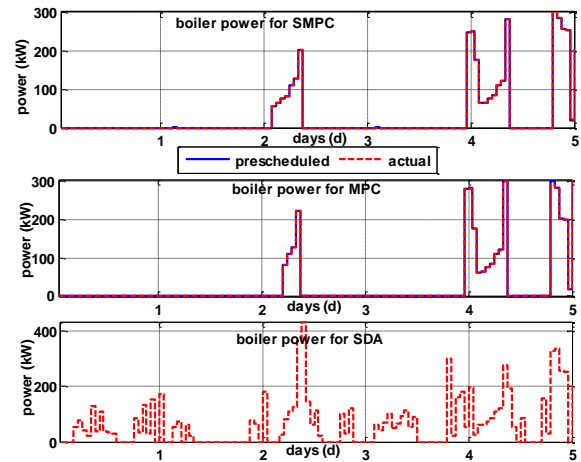


Fig. 8 Operation of boiler

The microgrid operation costs for the SMPC strategy, the MPC strategy and the SDA strategy are shown in Table 3. It shows that the SMPC strategy is the most robust control strategy: the total cost increment from the perfect forecast situation to the imperfect forecast situation for the SMPC strategy is lower than those for the MPC strategy and the SDA strategy. The microgrid total costs under perfect forecast situation for the SMPC strategy and the MPC

strategy are slightly lower than the SDA strategy, which is accounted for by the rolling horizon mechanism of the SMPC and the MPC strategies. In addition, the reason that the total cost of the SMPC strategy while taking into account of uncertainties (16474 \$) is also lower than the MPC strategy (17184 \$) lies in the fact that the SMPC strategy considers uncertainty conditions within the scenario based stochastic optimization model systematically in the prescheduling stage whereas the MPC strategy tackles the prescheduling stage problem only based on the point forecasts.

Table 3. Microgrid operation costs with SMPC strategy, MPC strategy and SDA strategy

	<i>SMPC strategy</i>	<i>MPC strategy</i>	<i>SDA strategy</i>
<i>Cost when considering forecast error</i>	16474 \$	17184 \$	18431 \$
<i>Cost when not considering forecast error</i>	16108 \$	16108 \$	16195 \$

6.2 Complexity and feasibility evaluation

The optimization problem in prescheduling operation stage is an NP problem, and its computational complexity mainly depends on the number of variables. We investigated the computational burden of the proposed optimization approach to be solved in each time interval, as shown in Table 4, in order to assess the feasibility of the proposed approach.

ILOG's CPLEX v.12 optimization solver is utilized to solve the optimization model given in Eq. (1) for the prescheduling optimization and also Eq. (56) for the real-time power compensation optimization. MATLAB 2013a and YALMIP toolbox are used for linking the CPLEX solver. All the computations are done on a PC with an Intel Core i5-640, 2.7 GHz CPU and 8 GB of RAM.

Table 4. Model statistics and computation times

<i>Approaches</i>	<i>Scenario reduction (s)</i>	<i>Number of variables</i>	<i>Mean solving time (s)</i>
<i>SMPC strategy</i>	9.72s	39942	23.53
<i>MPC strategy</i>	0	631	2.23
<i>SDA strategy</i>	9.72s	1684	3.41

There are 5000 initial (primary) scenarios generated by the Lattice Monte Carlo Simulation method (LMCS) to choose the typical scenarios. 20 typical scenarios are selected by the scenario selection method for the prescheduling stage optimization. The number of targeted typical scenarios are determined using stopping rules proposed in [35]. The number of variables in Table 4 is counted for both the prescheduling stage optimization and the real-time power stage optimization. The mean solving time represent the average solving time of each approach.

As Table 4 shows, the solution time of the SMPC strategy is relatively greater than other two strategies. However, it should be noted that such a solution time is negligible compared with normal sampling times (e.g., 1 hour in this study).

6.3 Impacts of fuel cell capacity

As the only device which connects the electrical subsystem and thermal subsystem, the fuel cell-based CHP generator plays an important role in the proposed CHP microgrid. In order to analyze the impacts of the fuel cell capacity on the microgrid operations, we consider four levels of CHP capacity, i.e. 300kW, 400kW, 500kW and 600kW, respectively. In addition, we assume perfect forecast in this subsection to focus on the impacts of different capacity levels of fuel cell. The operation schedules of boiler, TESS unit and fuel cell generator under each rated fuel cell capacity level (from 300 kW to 600kW) are shown in each column from left to right of Fig. 9.

It can be found that when the rated power capacity is 300kW, the fuel cell is operated frequently at its maximum power. The boiler and TESS also act as important roles to supply heat when the CHP generation is not enough.

When the fuel cell rate power becomes 400kW, it not only can supply heat to meet the thermal load in the microgrid but also take part in the energy trading in the electrical subsystem with the external power grid where the extra thermal energy is stored into the TESS.

When the fuel cell rate capacity becomes as high as 500kW or 600kW, no significant improvement (overall cost reduction) is observed, as shown in Table 5. This is mainly because the limited TESS capability limits the thermal power output of the CHP and therefore limits the electrical power production as well. This is also confirmed in Fig. 9.

Table 5. Microgrid operation costs under different fuel cell rate power

<i>Fuel cell rate power (kW)</i>	300	400	500	600
<i>Cost (\$)</i>	18274	16575	16295	16108

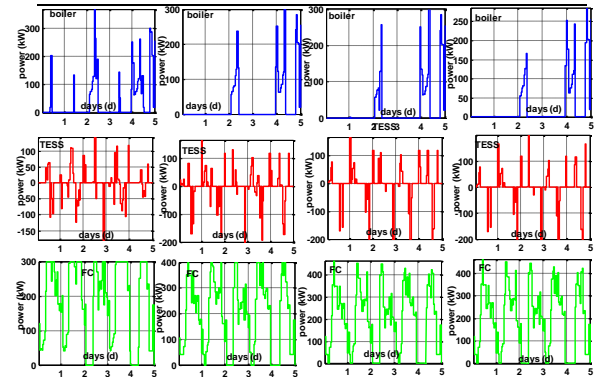


Fig. 9 Operation routines for boiler, TESS and fuel cell generator with different rated power of fuel cell.

6.4 Impacts of TESS capacity

As shown in Fig. 10, when the rated power of fuel cell is greater than 400kW, TESS usually charges and discharges at its maximum capability. As a result, the impacts of TESS capacity on microgrid operation are worth further investigation. In this subsection, three TESS power/energy capacity levels, i.e. 200kW/400kWh, 300kW/600kWh, and 400kW/800kWh are considered. Same as in the previous subsection, we assume perfect forecasts. The operation schedules of microgrid buying/selling, TESS and fuel cell are shown in Fig. 10.

It is observed from Fig. 10 that when the rated power and energy capacity of TESS increase, the maximum charge power of TESS increases at the same time. In addition, it is interesting to find out that the TESS always charges during time periods of high electricity prices, which indicates that the CHP is working in such time periods to produce extra electrical energy to sell back to the external grid to maximize the microgrid revenue. The surplus thermal energy generated by the CHP during these high price time periods is therefore stored into the TESS. The above can be seen in the microgrid buying/selling power routines in Fig. 10. In addition, the microgrid cost at different TESS capacity levels are shown in Table 6.

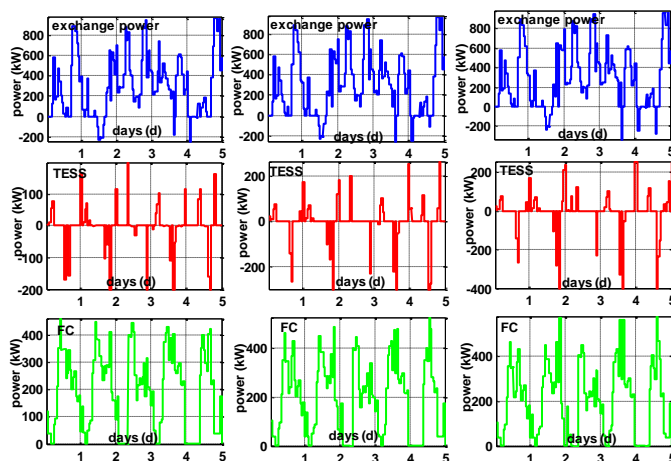


Fig. 10 Operation routines of microgrid buying/selling, TESS and fuel cell generator under different TESS capacity

Table 6. Microgrid operation cost with different rated fuel cell rated power

TESS capacity	200kW/	300kW/	400kW/
(kW/kWh)	400kWh	600kWh	800kWh
Cost (\$)	16108	16049	15843

7. Conclusion

In this study, a SMPC-based operation strategy to optimal control of a CHP microgrid is proposed. The microgrid consists of wind and PV environment-friendly generators, fuel cell based CHP generator and gas fired boiler units, energy storage devices (BESS and TESS) and many types of electrical and thermal loads. A two-stage microgrid control framework is proposed. The prescheduling stage is constructed by a scenario

based MILP model to minimize microgrid operation cost over the control horizon. The power compensation stage is constructed by solving a real-time economic dispatch model to coordinate dispatchable units which take part in the real-time operation. These two stages are implemented within a receding horizon control framework. Simulation results show that the SMPC-based microgrid operation strategy is more economic and robust compared to the traditional SDA-based microgrid operation strategy. In addition, the impacts of fuel cell and TESS rated capacities on system operations are discussed.

With respect to future studies, there are two directions that the present work can be further developed. First, the proposed model can be further developed in the view of a multi-objective optimization manner such as considering the carbon emissions as one of the optimization objectives. Second, we would like to extend the model to account for very large-scale problem cases and investigate an efficient, robust and scalable solution framework for such challenging problems.

Acknowledgment

This research is financially supported by National Natural Science Foundation of China (No. 61773390, 71671092), the key project of National University of Defense Technology (No. ZK18-02-09) and the Hunan Youth elite program (2018RS3081).

REFERENCES

- [1] Larsen G K H, van Foreest N D, Scherpen J M A. Distributed MPC applied to a network of households with micro-CHP and heat storage. *IEEE Transactions on Smart Grid*, 2014, 5(4): 2106-2114.
- [2] Guo L, Liu W, Cai J, et al. A two-stage optimal planning and design method for combined cooling, heat and power microgrid system. *Energy Conversion and Management*, 2013, 74: 433-445.
- [3] Arandian B, Ardehali M M. Effects of environmental emissions on optimal combination and allocation of renewable and non-renewable CHP technologies in heat and electricity distribution networks based on improved particle swarm optimization algorithm. *Energy*, 2017, 140: 466-480.
- [4] Nazari-Heris M, Abapour S, Mohammadi-Ivatloo B. Optimal economic dispatch of FC-CHP based heat and power micro-grids. *Applied Thermal Engineering*, 2017, 114: 756-769.
- [5] Bischi A, Taccari L, Martelli E, et al. A detailed MILP optimization model for combined cooling, heat and power system operation planning. *Energy*, 2014, 74: 12-26.
- [6] Kia M, Nazar M S, Sepasian M S, et al. Optimal day ahead scheduling of combined heat and power units with electrical and thermal storage considering security constraint of power system. *Energy*, 2017, 120:241-252.
- [7] Aghaei J, Alizadeh M I. Multi-objective self-scheduling of CHP (combined heat and power)-based microgrids considering demand response programs and ESSs (energy storage systems). *Energy*, 2013, 55: 1044-1054.
- [8] Nazari-Heris M, Abapour S, Mohammadi-Ivatloo B. Optimal Economic Dispatch of FC-CHP based Heat and Power Micro-grids. *Applied Thermal Engineering*, 2017(114): 756-769.
- [9] Bornapour M, Hooshmand R A, Parastegari M. An efficient scenario-based stochastic programming method for optimal scheduling of CHP-PEMFC, WT, PV and hydrogen storage units in micro grids. *Renewable energy*, 2019, 130: 1049-1066.
- [10] Zhang Y, Zhang T, Wang R, et al. Optimal operation of a smart residential microgrid based on model predictive control by considering uncertainties and storage impacts. *Solar Energy*, 2015, 122: 1052-1065.

- 1
2 [11] Sachs J, Sawodny O. A two-stage model predictive control strategy for
3 economic diesel-PV-battery island microgrid operation in rural areas.
4 IEEE Transactions on Sustainable Energy, 2016, 7(3): 903-913.
- 5 [12] Parisio A, Wiezorek C, Kyntäjä T, et al. Cooperative MPC-based energy
6 management for networked microgrids. IEEE Transactions on Smart
7 Grid, 2017, 8(6): 3066-3074.
- 8 [13] AFrancesca Verrilli, Seshadhri Srinivasan, Giovanni Gambino, et al.
9 Model Predictive Control-Based Optimal Operations of District Heating
10 System With Thermal Energy Storage and Flexible Loads. IEEE
11 Transactions on Automation Science and Engineering, 2017, 14(2):
12 547-557.
- 13 [14] Gu W, Wang Z, Wu Z, et al. An online optimal dispatch schedule for
14 CCHP microgrids based on model predictive control. IEEE transactions
15 on smart grid, 2017, 8(5): 2332-2342.
- 16 [15] Kriett P O, Salani M. Optimal control of a residential microgrid. Energy,
17 2012, 42(1): 321-330.
- 18 [16] Ramanunni P. Menon, François Marechal, Mario Paolone. Intra-day
19 electro-thermal model predictive control for polygeneration systems in
20 microgrids. Energy, 2016, 104: 308-319
- 21 [17] Luo Z, Wu Z, Li Z, et al. A two-stage optimization and control for CCHP
22 microgrid energy management. Applied Thermal Engineering, 2017, 125:
23 513-522.
- 24 [18] Su, W., Wang, J., & Roh, J. Stochastic energy scheduling in microgrids
25 with intermittent renewable energy resources. IEEE Transactions on
26 Smart Grid, 2014, 5(4), 1876-1883
- 27 [19] Parisio A, Rikos E, Glielmo L. Stochastic model predictive control for
28 economic/environmental operation management of microgrids: An
29 experimental case study. Journal of Process Control, 2016, 43: 24-37.
- 30 [20] Cominesi S R, Farina M, Giullioni L, et al. A two-layer stochastic model
31 predictive control scheme for microgrids. IEEE Transactions on Control
32 Systems Technology, 2018, 26(1): 1-13.
- 33 [21] Meibom, Peter; Barth, Rudiger; Hasche, Bernhard; et al. Stochastic
34 Optimization Model to Study the Operational Impacts of High Wind
35 Penetrations in Ireland. IEEE Transactions on Power Systems, 2011,
36 26(3): 1367-1379
- 37 [22] Doherty R, O'Malley M. A new approach to quantify reserve demand in
38 systems with significant installed wind capacity, IEEE Transactions on
39 Power Systems, 2005, 20(2): 587-595.
- 40 [23] Eduardo Arriagada, Enrique López, Miguel López, et al. A Stochastic
41 Economic Dispatch Model with Renewable Energies Considering
42 Demand and Generation Uncertainties. PowerTech (POWERTECH),
43 2013 IEEE Grenoble. IEEE, 2013: 1-6.
- 44 [24] Wu, L., M. Shahidehpour, and T. Li, Stochastic security-constrained unit
45 commitment. IEEE Transactions on Power Systems, 2007, 22(2):
46 800-811.
- 47 [25] Heitsch, H. and W. Römisch, Scenario reduction algorithms in stochastic
48 programming. Computational optimization and applications, 2003,
49 24(2-3): 187-206.
- 50 [26] Harikishan R. Ellamla, Iain Staffell, Piotr Bujlo, et al. Current status of
51 fuel cell based combined heat and power systems for residential sector,
52 Journal of Power Sources, 2015, 293: 312-328
- 53 [27] Alessandra Parisio, Evangelos Rikos, Luigi Glielmo. A Model Predictive
54 Control Approach to Microgrid Operation Optimization. IEEE
55 Transactions on Control Systems Technology, 2014, 22(5): 1813-1827.
- 56 [28] Dinghuan Zhu, Gabriela Hug. Decomposed Stochastic Model Predictive
57 Control for Optimal Dispatch of Storage and Generation. IEEE
58 Transactions on Smart Grid, 2014, 5(4): 2044-2053
- 59 [29] <http://www.elia.be/en/about-elia>
- 60 [30] Zhang D, Shah N, Papageorgiou L G. Efficient energy consumption and
61 operation management in a smart building with microgrid. Energy
62 Conversion and Management, 2013, 74: 209-222.
- 63 [31] Xu Y, Xie L, Singh C. Optimal scheduling and operation of load
64 aggregators with electric energy storage facing price and demand
65 uncertainties. North American Power Symposium (NAPS), 2011. IEEE,
2011: 1-7.
- [32] NYISO. <http://mis.nyiso.com/public/P-24Alist.htm>
- [33] Stluka, Petr, Godbole, Datta, Samad, Tariq. Energy management for
buildings and microgrids. In: 50th IEEE Conference on Decision and
Control and European Control Conference, 2011: 5150-5157.
- [34] Ozan Erdinc. Economic impacts of small-scale own generating and
storage units, and electric vehicles under different demand response
strategies for smart households. Applied Energy, 2014, 126: 142-150.
- [35] Siahkali, H., & Vakilian, M.. Stochastic unit commitment of wind farms
integrated in power system. Electric Power Systems Research, 80(9),
1006-1017.